

Medium-Entropy Alloy

Subjects: [Ergonomics](#)

Contributor: Da Hong , Hebin Wang , Longgang Hou , Ping Ou , Yiqi Wang , Hongjin Zhao

The objective of this study is to strengthen the FCC structured medium-entropy alloy using the hard carbides.

medium-entropy alloy

aging treatment

carbides

precipitation strengthening

1. Introduction

High-entropy alloys (HEAs) are defined as alloys composed of five or more principal elements with the molar ratio of each principal element between 5% and 35% [1]. As one of the new materials that developed in recent years, HEAs have received more and more attention [1][2][3][4][5][6][7][8][9][10][11][12] due to their unique property differences from traditional alloys for which the composition is based on one or two principal elements. HEAs are mainly manifested as the following four core effects: high configuration entropy in thermodynamics, sluggish atomic diffusion in kinetics, severe lattice distortion effect in structure, and “cocktail” effect in performance [4]. Due to their unique high-entropy effect, HEAs are easy to form a simple solid solution structure rather than intermetallic compounds, thus exhibiting high strength, high hardness, good ductility, and excellent thermal stability [13][14][15][16][17].

FeCoCrNi is a typical HEA with a simple face-centered cubic (FCC) structure, possessing good ductility and fracture toughness at room temperature or liquid nitrogen temperature. However, its strength is only 145 MPa in the as-cast state, which is far from meeting the demand of practical applications [18]. In order to solve this issue, some strengthening methods, such as fine grain strengthening, dislocation strengthening, precipitation strengthening, and solution strengthening should be introduced into this alloy. Among them, precipitation strengthening is an effective method to improve the strength of FeCoCrNi HEA. T T shun et al. [19] have investigated the aging-hardening of the FeCoCrNiMo_{0.85} HEA after aging at 700–1000 °C, and they found that the σ phase can be completely transformed into the μ phase after 700 °C aging, giving rise to the hardness increasing from 420 to 621 HV. He et al. [20] have studied the strengthening mechanism of FCC precipitates in CoCrFeNiNb_{0.25} HEA and found that FCC precipitates appeared in the matrix after annealing, resulting in doubling the strength without losing the plasticity. As interstitial atoms, carbon is widely used in the traditional structural materials such as steels and super-alloys due to its solid solution strengthening and carbide precipitation strengthening [21][22][23][24]. In some super-austenitic steel, the precipitation of carbide in the austenitic matrix can give rise to the outstanding strength at high temperatures. Ou et al. [25][26] observed that the dense nanosized MX phases were precipitated at the coherent Cu-rich phase with a nanosized diameter in the austenitic matrix, contributing an excellent precipitation strengthening effect and creep resistance in the Super304H austenitic steel. Anburaj et al. [27] investigated the precipitation behavior in an aged super-austenitic stainless steel and found that

chi, carbides, and sigma phases are formed during aging at 500–1000 °C, giving rise to the increase in the hardness, while the incoherent sigma precipitate in the austenite matrix was detrimental to the toughness of alloys. In recent years, carbons have already been applied in HEAs gradually. Wu et al. [28] have reported that both the yield strength and the tensile strength of CoCrFeNiMnHEA were significantly increased by adding 0.5 at.% of C. N. Gao et al. [29] have studied the strengthening effect of NbC precipitation on the microstructure and property of FeCoCrNiMn HEA and found that 0.8 at.% of Nb/C addition can increase the yield strength and ultimate tensile strength to 732 MPa and 911 MPa, respectively, while maintaining a high elongation of 32%.

Many studies have shown that equal atomic ratios are not the necessary condition for the formation of single-phase solid solutions. For example, Tasan et al. [30] have investigated the effect of non-equal atomic ratios on the phase stability, deformation mechanism, and mechanical properties of FeCoCrNiMn HEA, and they found that the $\text{Fe}_{40}\text{Mn}_{27}\text{Ni}_{26}\text{Co}_5\text{Cr}_2$ alloy is composed of a stable single FCC structure, and the quaternary unequal atomic ratio $\text{Fe}_{37}\text{Mn}_{45}\text{Co}_9\text{Cr}_9$ alloy is also comprised of a single FCC equiaxed crystal structure after homogenization treatment. Ma et al. [31] have found that the $\text{Fe}_{42}\text{Cr}_{20}\text{Ni}_{30}\text{Co}_6\text{Cr}_2$ MEA contains only a single FCC phase. Stepanov et al. [32] have studied a series of quaternary Cr–Fe–Ni–Mn non-equal atomic ratio alloys, and they found that the $\text{Fe}_{40}\text{Mn}_{28}\text{Ni}_{28}\text{Cr}_4$, $\text{Fe}_{40}\text{Mn}_{28}\text{Ni}_{20}\text{Cr}_{12}$, and $\text{Fe}_{40}\text{Mn}_{28}\text{Ni}_{14}\text{Cr}_{18}$ alloys are all composed of a simple FCC structure.

Carbides are an effective hardening particle for improving the strength of the steels. For example, Scott et al. [33] have enhanced the strength of high manganese austenitic TWIP steels by TiC, NbC, and VC. Wang et al. [34] found that the ultrafine M_3C , M_7C_3 , and M_{23}C_6 carbides are responsible for the enhanced strength of high chromium steels. VC and Mo_2C are hard phases with simple crystal structures, which are commonly formed in V-Mo-containing steels. VC/ Mo_2C carbides usually show two main types of size distribution: one is the primary carbides with a size range of 1–10 μm formed during solidification, and the other is the fine strengthening secondary precipitates with a nanometer size generated from a supersaturated matrix during the aging treatment or when the steels are serviced at high temperature. The substantial strengthening effect of VC/ Mo_2C carbides has been reported for various steel grades [35][36]. So far, few have rarely reported on the precipitation behavior of Mo_2C , VC, Cr_7C_3 , etc., in FeCoCrNiHEAs, although these particles can be used to strengthen the alloy by second phase strengthening. Therefore, the purpose of this work is to use the hard Mo_2C and VC carbides to strengthen FCC-structured HEA using a high content of carbide-forming elements. There are two considerations that need to be taken into account when designing the alloy composition. Firstly, increasing the Fe content to above 50% on the basis of FeCoCrNi HEA can effectively reduce the cost of HEAs while still obtaining adequate entropy configuration to stabilize FCC solid solution over intermetallic compounds. Secondly, strong carbide-forming elements Mo and V and sufficient C element are added for promoting the precipitates of carbides. The investigated alloy is named as non-equal-atomic $\text{Fe}_{55}(\text{CoCrNi})_{10}(\text{MoV})_5\text{C}_5$, which can be classified as a medium-entropy alloy (MEA), according to the generally accepted definition that specifies MEA as an alloy with the configuration entropy between R and 1.5R, in which R is the gas constant.

2. Tensile Properties

Figure 1 shows the engineering stress-strain curves of the alloys in different states. It can be seen that the tensile strength and elongation of the as-cast alloy was low. When the alloy was aged, both the ductility and strength increased. The mechanical properties of the alloys in different states are collected in Table 1. As can be shown, the tensile strength of the alloy reached a maximum value of 626 MPa after aging at 800 °C for 4 h, which increased by 94% compared to those of the as-cast alloy, while the elongation increased from 1.2% to 6.2%. As the temperature increases to 1000 °C, its tensile strength decreased to 548 MPa, and the elongation decreased to 2.9%. Figure 2 shows the tensile fracture morphology of the alloys at different states. As shown in Figure 2a,b, the fracture surface of the as-cast alloy is characterized by cleavage facets, secondary cracks, and a small amount of tearing ridges, suggesting that it belongs to brittle fracture. This is because there are a large number of network carbides on the grain boundary, which can seriously reduce the plasticity of the alloy. Figure 2c,d show the fracture morphology of the alloy after aging at 800 °C for 4 h, and it can be found that there are more tearing edges and increased dimples except for some river-like cleavage facets, indicating that the fracture mechanism belongs to quasi-cleavage fracture. The improvement of ductility for the 800 °C aged alloy might be attributed to the large number of carbide particles dispersed throughout the matrix effectively released local stress concentration during deformation, thus making the cracks difficult to initiate and propagate. On the other hand, the precipitation of the secondary phase particles can promote the nucleation of microscopic voids and the occurrence of local plastic deformation, thus increasing elongation [37]. The fracture morphology of the 1000 °C aged alloy shown in Figure 2e,f manifests a complex fracture surface of river-like cleavage facets, cleavage steps, and a few dimples, indicating that the type of fracture belongs to brittle fracture. As depicted above, the fine precipitates have coarsening and aggregating after being aged at 1000 °C. Some studies have pointed out that the larger carbides can weaken the effect of the precipitation strengthening, leading to the decrease in strength [38][39]. As the VC carbides grow up, a stress concentration is generated around them during the deformation process, and the crack is easy to form and expand, thus reducing the ductility.

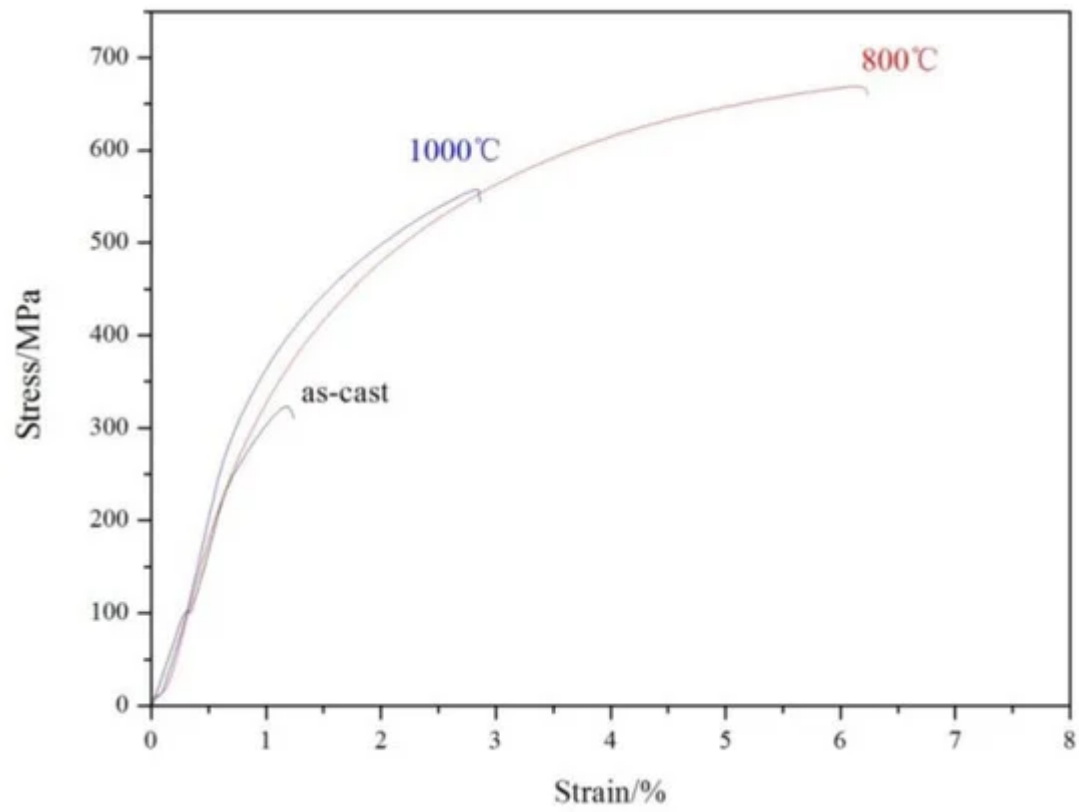


Figure 1. Engineering stress-strain curves of the alloys in different states.

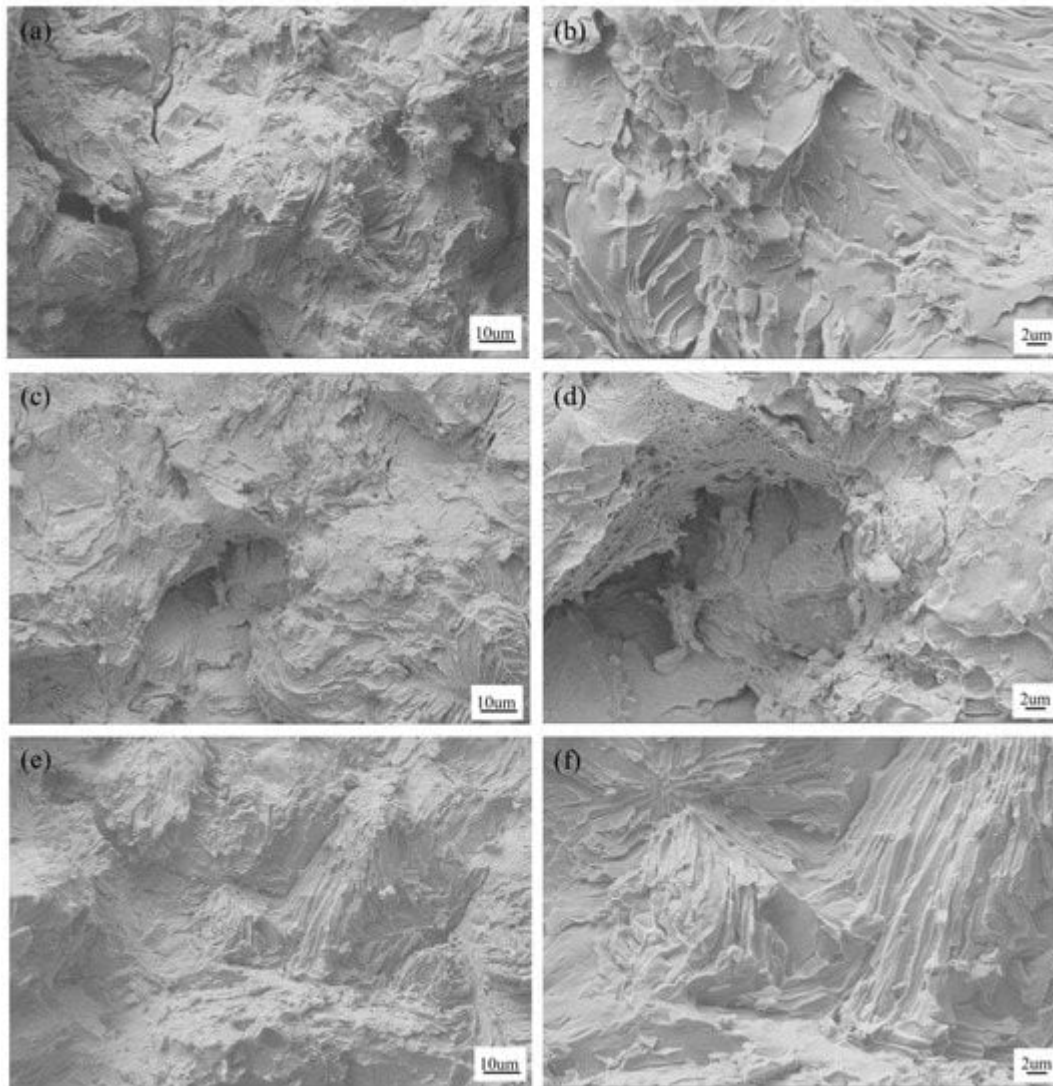


Figure 2. The fracture morphologies of the investigated alloys: (a,b) as-cast; (c,d) 800 °C aged for 4 h; (e,f) 1000 °C aged for 4 h.

Table 1. Yield strength, ultimate tensile strength, and elongation of alloys in different states.

States	Yield Strength σ_y /MPa	Ultimate Tensile Strength σ_b /MPa	Elongation ϵ /%
As-cast	313	322	1.2

References

1. Yeh, J.W.; Chen, S.K.; Lin, S.J.; Gan, J.Y.; Chin, T.S.; Shun, T.T.; Tsau, C.H.; Chang, S.Y. Nanostructured high-entropy alloys with multiple principal elements: Novel alloy design concepts and outcomes. *Adv. Eng. Mater.* 2004, 6, 299–303.
2. Miracle, D.B.; Senkov, O.N. A critical review of high entropy alloys and related concepts. *Acta Mater.* 2017, 122, 448–511.
3. Ye, Y.F.; Wang, Q.; Lu, J.; Liu, C.T.; Yang, Y. High-entropy alloy: Challenges and prospects. *Mater. Today* 2016, 19, 349–362.
4. Zhang, Y.; Zuo, T.T.; Tang, Z.; Gao, M.C.; Dahmen, K.A.; Liaw, P.K.; Lu, Z.P. Microstructures and properties of high-entropy alloys. *Prog. Mater. Sci.* 2014, 61, 1–93.
5. He, F.; Wang, Z.; Wu, Q.; Niu, S.; Li, J.; Wang, J.; Liu, C.T. Solid solution is land of the Co-Cr-Fe-Ni high entropy alloy system. *Scr. Mater.* 2017, 131, 42–46.
6. Zhang, W.R.; Liaw, P.K.; Zhang, Y. Science and technology in high-entropy alloys. *Sci. China Mater.* 2018, 61, 2–22.
7. Wang, W.R.; Wang, W.L.; Wang, S.C.; Tsai, Y.C.; Lai, C.H.; Yeh, J.W. Effects of Al addition on the microstructure and mechanical property of $\text{Al}_x\text{CoCrFeNi}$ high-entropy alloys. *Intermetallics* 2012, 26, 44–51.
8. Li, Z.; Pradeep, K.G.; Deng, Y.; Raabe, D.; Tasan, C.C. Metastable high-entropy dual-phase alloys overcome the strength-ductility trade-off. *Nature* 2016, 534, 227–230.
9. Stepanov, N.D.; Shaysultanov, D.G.; Chernichenko, R.S.; Yurchenko, N.Y.; Zherebtsov, S.V.; Tikhonovsky, M.A.; Salishchev, G.A. Effect of thermomechanical processing on microstructure and mechanical properties of the carbon-containing CoCrFeNiMn high entropy alloy. *J. Alloys Compd.* 2017, 693, 394–405.
10. Qiu, X.W.; Wu, M.J.; Liu, C.G.; Zhang, Y.P.; Huang, C.X. Corrosion performance of $\text{Al}_2\text{CrFeCo}_x\text{CuNiTi}$ high-entropy alloy coatings in acid liquids. *J. Alloys Compd.* 2017, 708, 353–357.
11. Seol, J.B.; Bae, J.W.; Li, Z.; Han, J.C.; Kim, J.G.; Raabe, D.; Kim, H.S. Boron doped ultrastrong and ductile high-entropy alloys. *Acta Mater.* 2018, 151, 366–376.
12. Riva, S.; Tudball, A.; Mehraban, S.; Lavery, N.P.; Brown, S.G.R.; Yuseenko, K.V. A novel High-Entropy Alloy-based composite material. *J. Alloys Compd.* 2018, 730, 544–551.
13. Lin, C.M.; Tsai, H.L.; Bor, H.Y. Effect of aging treatment on microstructure and properties of high-entropy $\text{Cu}_{0.5}\text{CoCrFeNi}$ alloy. *Intermetallics* 2010, 18, 1244–1250.
14. Ren, B.; Liu, Z.X.; Li, D.M.; Shi, L.; Cai, B.; Wang, M.X. Corrigendum to “Effect of elemental interaction on microstructure of CuCrFeNiMn high-entropy alloy system”. *J. Alloys Compd.* 2010, 503, 538–538.

15. Tsai, K.Y.; Tsai, M.H.; Yeh, J.W. Sluggish diffusion in Co–Cr–Fe–Mn–Ni high-entropy alloys. *Acta Mater.* 2013, 61, 4887–4897.
16. Chuang, M.H.; Tsai, M.H.; Wang, W.R.; Lin, S.J.; Yeh, J.W. Microstructure and wear behavior of Al_xCo_{1.5}CrFeNi_{1.5}Ti_y high-entropy alloys. *Acta Mater.* 2011, 59, 6308–6317.
17. Li, X.F.; Feng, Y.H.; Liu, B.; Yi, D.H.; Yang, X.H.; Zhang, W.D.; Chen, G.; Liu, Y.; Bai, P.K. Influence of NbC particles on microstructure and mechanical properties of AlCoCrFeNi high-entropy alloy coatings prepared by laser cladding. *J. Alloys Compd.* 2019, 788, 485–494.
18. Jiang, H.; Han, K.M.; Qiao, D.X.; Lu, Y.P.; Chao, Z.Q.; Li, T.J. Effects of Ta Addition on the Microstructures and Mechanical Properties of CoCrFeNi High Entropy Alloy. *Mater. Chem. Phys.* 2018, 210, 43–48.
19. Shun, T.T.; Chang, L.Y.; Shiu, M.H. Age-hardening of the CoCrFeNiMo_{0.85} high-entropy alloy. *Mater. Charact.* 2013, 81, 92–96.
20. He, F.; Wang, Z.J.; Liu, S.Z.; Wu, Q.F.; Li, J.J.; Wang, J.C.; Liu, C.T.; Dang, Y.Y. Strengthening the CoCrFeNiNb_{0.25} high entropy alloy by FCC precipitate. *J. Alloys Compd.* 2016, 667, 53–57.
21. Saenarjhan, N.; Kang, J.H.; Kim, S.J. Effects of carbon and nitrogen on austenite stability and tensile deformation behavior of 15Cr-15Mn-4Ni based austenitic stainless steels. *Mater. Sci. Eng. A.* 2019, 742, 608–616.
22. Conrad, H. Effect of interstitial solutes on the strength and ductility of titanium. *Prog. Mater. Sci.* 1981, 26, 123–403.
23. Urrutia, I.G.; Raabe, D. Multistage strain hardening through dislocation substructure and twinning in a high strength and ductile weight-reduced Fe-Mn-Al-C steel. *Acta Mater.* 2012, 60, 5791–5802.
24. Gutierrez, I.; Raabe, D. Microbanding mechanism in a Fe-Mn-C high-Mn twinning-induced plasticity steel. *Scr. Mater.* 2013, 69, 53–56.
25. Ou, P.; Xing, H.; Sun, J. Precipitation of nanosized MX at coherent Cu-rich phases in Super304H austenitic steel. *Metall. Mater. Trans. A.* 2015, 46, 1–5.
26. Ou, P.; Li, L.; Xie, X.F.; Sun, J. Steady-state creep behavior of Super304H austenitic steel at elevated temperatures. *Acta Metall. Sin. (Engl. Letters)* 2015, 28, 1336–1343.
27. Anburaj, J.; Nazirudeen, S.S.M.; Narayanan, R.; Anandavel, B.; Chandrasekar, A. Ageing of forged superaustenitic stainless steel: Precipitate phases and mechanical properties. *Mater. Sci. Eng. A.* 2012, 535, 99–107.
28. Wu, Z.; Parish, C.M.; Bei, H. Nano-twin mediated plasticity in carbon-containing FeNiCoCrMn high entropy alloys. *J. Alloys Compd.* 2015, 647, 815–822.

29. Gao, N.; Lu, D.H.; Zhao, Y.Y.; Liu, X.W.; Liu, G.H.; Wu, Y.; Liu, G.; Fan, Z.T.; Lu, Z.P.; George, E.P. Strengthening of a CrMnFeCoNi high-entropy alloy by carbide precipitation. *J. Alloys Compd.* 2019, 792, 1028–1035.
30. Tasan, C.C.; Deng, Y.; Pradeep, K.G.; Yao, M.J.; Springer, H.; Raabe, D. Composition Dependence of Phase Stability, Deformation Mechanisms, and Mechanical Properties of the CoCrFeMnNi High-Entropy Alloy System. *JOM* 2014, 66, 1993–2001.
31. Ma, D.C.; Yao, M.J.; Pradeep, K.G.; Tasan, C.C.; Springer, H.; Raabe, D. Phase stability of non-equiatomically CoCrFeMnNi high entropy alloys. *Acta Mater.* 2015, 98, 288–296.
32. Stepanov, N.D.; Shaysultanov, D.G.; Tikhonovsky, M.A.; Salishchev, G.A. Tensile properties of the Cr-Fe-Ni-Mn non-equiatomically multicomponent alloys with different Cr contents. *Mater. Des.* 2015, 87, 60–65.
33. Scott, C.; Remy, B.; Collet, J.L.; Cael, A.; Bao, C.; Danoix, F.; Malard, B.; Curfs, C. Precipitation strengthening in high manganese austenitic TWIP steels. *Int. J. Mater. Res.* 2011, 102, 538–549.
34. Wang, Y.; Li, M.Y.; Han, B.; Han, T.; Cheng, Y.Y. Influence of secondary carbides precipitation and transformation on the secondary hardening of laser melted high chromium steel. *J. Mater. Sci.* 2010, 45, 3442–3447.
35. Xu, W.; Rivera-Diaz-del-Castillo, P.E.J.; Yan, W.; Yang, K.; Martin, D.S.; Kestens, L.A.I.; van der Zwaag, S. A new ultrahigh-strength stainless steel strengthened by various coexisting nanoprecipitates. *Acta Mater.* 2010, 58, 4067–4075.
36. Wang, H.B.; Hou, L.G.; Li, Y.B.; Ou, P.; Shen, L.; Wen, X.E.; Cui, H.; Zhang, J.S. Effect of niobium on the secondary precipitates and tempering resistance of spray-formed M3:2 high-speed steel. *J. Mater. Eng. Perform.* 2019, 28, 926–937.
37. Zhong, Q.P.; Zhao, Z.H. *Fractography*; Higher Education Press: Beijing, China, 2006.
38. Kamikawa, N.; Abe, Y.; Miyamoto, G.; Funakawa, Y.; Furuhashi, T. Erratum to “Tensile Behavior of Ti, Mo-added Low Carbon Steels with Interphase Precipitation”. *ISIJ Int.* 2014, 54, 212–221.
39. Hao, L.H.; Ji, X.; Zhang, G.Q.; Zhao, W.; Sun, M.Y.; Peng, Y. Carbide precipitation behavior and Mechanical properties of micro-alloyed medium Mn steel. *J. Mater. Sci. Technol.* 2020, 47, 122–130.

Retrieved from <https://encyclopedia.pub/entry/history/show/4081>